

Accelerated growth in the absence of DNA replication origins

Michelle Hawkins^{#1}, Sunir Malla², Martin J. Blythe², Conrad A. Nieduszynski^{#1}, and Thorsten Allers^{#1}

¹School of Biology, University of Nottingham, Queen's Medical Centre, Nottingham, NG7 2UH, UK.

²DeepSeq, University of Nottingham, Queen's Medical Centre, Nottingham, NG7 2UH, UK.

These authors contributed equally to this work.

Abstract

DNA replication initiates at defined sites called origins, which serve as binding sites for initiator proteins that recruit the replicative machinery. Origins differ in number and structure across the three domains of life¹ and their properties determine the dynamics of chromosome replication. Bacteria and some archaea replicate from single origins, whilst most archaea and all eukaryotes replicate using multiple origins. Initiation mechanisms that rely on homologous recombination operate in some viruses. Here we show that such mechanisms also operate in archaea. We have used deep sequencing to study replication in *Haloferax volcanii*. Four chromosomal origins of differing activity were identified. Deletion of individual origins resulted in perturbed replication dynamics and reduced growth. However, a strain lacking all origins has no apparent defects and grows significantly faster than wild-type. Origin-less cells initiate replication at dispersed sites rather than at discrete origins and have an absolute requirement for the recombinase RadA, unlike strains lacking individual origins. Our results demonstrate that homologous recombination alone can efficiently initiate the replication of an entire cellular genome. This raises the question of what purpose replication origins serve and why they have evolved.

Haloferax volcanii is a genetically-tractable archaeon^{2,3}, its 2.85 Mb main chromosome is replicated from multiple origins⁴ using machinery homologous to that found in eukaryotes¹. To characterize replication dynamics in *H. volcanii*, we generated replication profiles by deep sequencing the wild isolate DS2 and laboratory strain H26 (Supplementary Table 1). Read counts from asynchronous replicating cells were normalized to non-replicating cells (Extended Data Fig. 1)⁵. Peaks in relative copy number correspond to sequences that are over-represented in replicating cells and therefore identify active origins (Fig. 1). In the wild isolate DS2, peaks at 0 and 1593 kb of the main chromosome co-localize with previously described origins (*oriC1* and *oriC2*, respectively), as do peaks in the mega-plasmid profiles (Extended Data Fig. 2)⁴. The peak at 571 kb represents a third chromosomal origin, *oriC3* (Extended Data Fig. 3). Unlike *oriC1* and *oriC2*, *oriC3* is not situated at a nucleotide skew inflection point⁴; in bacteria and archaea, such inflection points reflect origin usage over

Correspondence and requests for materials should be addressed to TA: thorsten.allers@nottingham.ac.uk and CAN: conrad.nieduszynski@nottingham.ac.uk.

Author Contributions: MH, CAN and TA contributed equally to this work. MH, CAN and TA conceived and designed experiments; MH and TA performed experiments; SM prepared libraries for sequencing; MB aligned sequencing data to the genome; CAN analysed sequencing data; MH, CAN and TA interpreted results and wrote the paper.

Extended Data and Supplementary Information is also available in the online version of the paper.

Author Information: Sequencing data have been submitted to NCBI Gene Expression Omnibus under accession number GSE41961. Reprints and permissions information are available at <http://www.nature.com/reprints>. The authors declare no competing interests. Readers are welcome to comment on the online version of the paper.

evolutionary timescales⁶. This is consistent with infrequent use of *oriC3* or the recent acquisition of an origin at this location.

The sharp peaks reflect discrete origins, whereas the smooth valleys represent broad zones of termination⁷. Broad termination zones (as opposed to specific termination sites) have been described in other archaea⁸ and in eukaryotes^{7,9}, suggesting they are a feature of chromosomes with multiple origins. The variable peak heights indicate that the chromosomal origins differ in activity, this interpretation is supported by mathematical modeling (A. de Moura, personal communication) and plasmid-based assays (Extended Data Fig. 3c). Such a functional hierarchy of origins may be due to different usage and/or activation times^{9,10}.

Laboratory strain H26 shows discontinuities in the replication profiles of the main chromosome and mega-plasmid pHV4 (at 249 and 286 kb respectively; Fig. 1b). Discontinuities indicate substantial differences in replication time between adjacent regions and suggest genome rearrangements¹¹. We determined this rearrangement to be integration of pHV4 into the main chromosome (Fig. 1c, 1d and Extended Data Fig. 4). Remapping the data to a reconstructed genome sequence results in a continuous profile (Fig. 1c and 3a). The additional peak at 535 kb corresponds to the integrated pHV4 origin, *ori-pHV4*.

If an origin is active in all cells and used only once per generation, the ratio of origin to terminus regions cannot exceed 2:1; values of >2:1 are only possible if concurrent rounds of replication are initiated. The ratio of the wild isolate is 2:1 (Fig. 1a), but exceeds 2:1 for H26 (Fig. 1c and 3a). This is consistent with concurrent rounds of replication and precludes the existence of alternating phases of replication and segregation in *H. volcanii* (in contrast to eukaryotes and crenarchaea such as *Sulfolobus*¹²). Therefore, regulated timing of origin activation is unlikely and the peak height differences we observe are probably due to differences in origin usage.

We tested the requirement for origins by chromosomal deletion in strain H26 (hereafter designated wild-type). All combinations of origin deletion resulted in viable strains, including a strain deleted for all four chromosomal origins (Fig. 2a). Deletion of individual origins led to minor changes in DNA content (notably $\Delta oriC3$), but the strain lacking all chromosomal origins had a DNA content profile indistinguishable from wild-type (Fig. 2b). We used pairwise growth competition to quantify strain fitness (Fig. 2c). Single origin deletion strains grew slower than wild-type, with strains lacking *oriC3* exhibiting the greatest growth defect. Surprisingly, the strain deleted for all four origins grew 7.5% faster than wild-type, and the strain lacking the three most active origins (*oriC1,2,3*) grew 5.5% faster (Fig. 2c). In fact, growth rate correlates inversely with the activity of remaining origins. For example, the $\Delta oriC2,3$ strain retains the most active origin *oriC1* and has a 0.8% growth defect, whereas the $\Delta oriC1,2$ strain has lost the two most active origins and has a 2.3% growth advantage.

How could genome replication be maintained despite the deletion of all chromosomal origins? Deletion of known origins might reveal dormant origins as seen in yeast^{13,14}. Alternatively, replication could initiate independently of canonical origins, with little or no site specificity. To distinguish between these possibilities, we profiled replication in the origin deletion strains (Fig. 3, Supplementary Table 1). The peaks associated with deleted origin(s) are no longer evident and there are no new discrete peaks. The minima have relocated indicating that there are no enforced termination sites. The profiles of strains deleted for all (or the three most active) origins show a zone of copy number enrichment near the $\Delta oriC2$ locus (Fig. 3e and f; ~2230 kb). However, this does not resemble the sharp

peaks associated with characterized origins (Fig. 1 and 3a). Therefore, we find no evidence for activation of dormant origins.

Instead, the profiles are consistent with origin-independent initiation. In contrast to the sharp peaks observed in the wild-type, profiles of the single origin deletion strains exhibit global flattening that has rounded the remaining peaks (Fig. 3b-d); the minima at termination zones are also shallower. Sharp peaks indicate discrete origin sites, therefore peak flattening is a consequence of replication initiation at dispersed sites. The profiles of strains deleted for all (or the most active) origins are largely flat, consistent with widespread origin-independent initiation (Fig. 3e and f).

We considered two mechanisms for dispersed initiation. Origins are binding sites for the initiator protein ORC1; in the absence of origins, ORC1 could bind non-specifically throughout the genome¹⁵. Alternatively, dispersed initiation could rely upon homologous recombination. Origin-independent replication can occur when recombination (D-loop) or transcription (R-loop) intermediates are used to prime replication^{16,17}. We note that in strains deleted for all or the most active origins, the zone of copy number enrichment at ~2230 kb is near the *rrnB* rRNA operon (Fig. 3e and f; 2234-2239 kb). Highly transcribed DNA is associated with elevated recombination levels¹⁸, therefore D-loops and R-loops in the *rrnB* region could facilitate replication initiation. This is analogous to recombination-dependent replication in viruses¹⁷ and to DNA damage-inducible replication in *Escherichia coli*. The latter is known as ‘stable DNA replication’ and occurs in the absence of *oriC* or the initiator protein DnaA; instead it relies on recombination catalyzed by RecA to initiate replication¹⁶.

H. volcanii mutants lacking RadA (the archaeal RecA/Rad51 homologue) are viable but defective in recombination. Unlike RecA, RadA does not have a secondary role in activating an SOS response¹⁹. However, RadA is essential for the replication of pHV2-based plasmids, which do not use ORC-based initiation²⁰. We attempted to delete *radA* from the origin deletion strains using established methods²¹. This was successful in the wild-type and single origin deletion strains, but only a single $\Delta oriC1,2,3 \Delta radA$ isolate was recovered; this strain had undergone a chromosomal rearrangement involving *ori-pHV4* (Extended Data Fig. 5). We were unable to delete *radA* from the strain lacking all four origins, indicating that recombination is essential in the absence of replication origins. To confirm this, we placed *radA* under control of a tryptophan-inducible promoter (Extended Data Fig. 6)²². In the absence of tryptophan, when this promoter is tightly repressed, wild-type cells with inducible *radA* are viable whereas origin-less cells fail to grow (Fig. 4).

Work by Kogoma¹⁶ showed that *E. coli oriC* mutants can use homologous recombination to initiate replication. However these cells exhibit profound growth defects²³. In contrast, origin-less strains of *H. volcanii* grow faster than wild-type. Furthermore, recombination-dependent replication in *E. coli* is only possible in strains harboring suppressor mutations (e.g. *sdrA*, which stabilizes R-loops by inactivating RNaseH¹⁶). We found no mutations in any of the four *H. volcanii* RNaseH genes. Only five single nucleotide polymorphisms (SNPs) were identified in the strain lacking all origins, and all of these SNPs are already present in the respective parent strains (Extended Data Table 1). Therefore, we find no evidence for suppressors, akin to those reported by Kogoma²³, which are required for growth in the absence of origins.

Our results indicate that it is possible to replicate an entire genome by recombination-dependent initiation alone, with no apparent cost to fitness. How might this be accomplished? In wild-type, binding of ORC1 at origins leads to recruitment of the replicative helicase MCM, which may be rate-limiting for initiation¹. In the single origin

deletion strains, liberation of MCM from deleted origins could stimulate recombination-dependent initiation, resulting in flattening of the replication profiles (Fig. 3b-d). We postulate that the activity of origins correlates with their affinity for MCM. Therefore, deleting an active origin (*oriC1*) liberates more MCM than deleting a weak origin (*oriC3*). This liberated MCM is recruited to D-loops and used to initiate recombination-dependent replication. Our observation that growth rate correlates inversely with the activity of remaining origins (Fig. 2c) suggests that recombination-dependent replication is more efficient than origin-dependent replication, but the former has a lower affinity for MCM. Consistent with this, *Pyrococcus abyssi* MCM is recruited to both the origin and a region containing rRNA and tRNA genes; the latter becomes the major binding site in stationary phase, suggesting liberation of MCM from the origin²⁴.

What then is the purpose of replication origins? It is assumed that regularly-spaced origins ensure genome duplication in the shortest possible time²⁵. This assumption is challenged by our data showing that origin-less cells grow faster than wild-type. Alternatively, defined origins can be used to co-ordinate the direction of replication with the orientation of highly-expressed genes. Collisions between replication and transcription machineries can stall DNA replication, and restarting stalled forks by recombination entails a risk of genome rearrangements. We did not observe any such rearrangements, except when the Δ *oriC1,2,3* strain was challenged with inactivation of recombination (Extended Data Fig. 5). Moreover, the rapid growth of origin-less mutants suggests that collisions between replication and transcription are less problematic than assumed.

Regulated initiation at origins allows for coordination of genome replication with segregation. This is critical in organisms with tightly-regulated ploidy, such as *E. coli*, *Sulfolobus* and most eukaryotes¹². However, *H. volcanii* is highly polyploid, tolerates variation in genome copy number²⁶ and there is no evidence for a regulated cell cycle (I. Duggin, personal communication). We suggest that the high ploidy of *H. volcanii* enables the accelerated growth of origin-less strains, in contrast to the growth defects observed in *E. coli*²³. With a ploidy of 20, *H. volcanii* can rely on stochastic partitioning to ensure that daughter cells inherit a genome complement. However, it is vital that these 20 genome sequences are equalized to prevent the accumulation of recessive mutations, and this requires efficient recombination. In yeast, a screen for gene deletions that are lethal in polyploid cells found that almost all such mutations affect genomic stability, notably by impairing recombination²⁷. Therefore, polyploidy creates a situation (in yeast) where homologous recombination becomes essential; it follows that naturally polyploid organisms such as *H. volcanii* are heavily reliant upon recombination. Indeed, *radA* mutants of *H. volcanii* suffer a more severe growth defect than *recA* mutants of *E. coli*²⁰.

In *H. volcanii*, origin-dependent initiation of replication appears to offer no demonstrable advantage; however, cells lacking individual origins are disadvantaged. We propose that origins are selfish genetic elements that ensure their own replication. Over time, origins become integrated with cellular processes such as the cell cycle, to coordinate genome duplication, segregation and cell division; ultimately this results in reduced ploidy. Propagation of selfish elements within a population requires a sexual process and lateral gene transfer by cell mating has been observed in *H. volcanii*²⁸. It is notable that most archaeal origins are adjacent to the gene for their cognate initiator protein ORC1¹. Such tight linkage, which is typical of selfish elements, ensures that origins acquired by lateral gene transfer can successfully subvert the replicative machinery of their host. This is known as the replicon takeover hypothesis, where the host cell chromosome becomes dependent on extra-chromosomal elements for its propagation²⁹. The replicon takeover hypothesis has until now focused on the DNA replication apparatus, but our findings suggest that origins can also behave as selfish genetic elements.

Methods

Reagents

Strains, plasmids, oligonucleotides and probes are given in Extended Data Tables 2-4. *H. volcanii* was grown as described previously³⁰. Pairwise growth competition assays were carried out as described previously²¹, except that wild-type and mutant strains were mixed in a 1:1 ratio (for further details see Source Data for Fig. 2c). Tryptophan gradient agar plates³¹ were cast from a tapered wedge of Hv-Ca agar³⁰ containing 0.25 mM tryptophan, which was overlaid with a converse wedge of Hv-Ca agar.

Molecular genetic methods

Transformation of *H. volcanii* and genomic deletions were carried out as described previously³⁰. Standard molecular techniques were used, pulsed field gels were carried out as described previously²¹. Genomic DNA for deep sequencing was isolated from 100 ml Hv-YPG culture in stationary phase (A650 >1) or 1 L in exponential phase (A650 ~0.1) as described previously³⁰, followed by phenol:chloroform extraction. For flow cytometry, live cells in exponential phase (A650 ~0.1) were stained with acridine orange and immediately analyzed using an Apogee A40 as described previously^{26,32}; 50000 cells were counted, doublet signals were removed by gating on peak/area plots and data analyzed using FlowJo (TreeStar Inc.).

SOLiD sequencing and data analysis

Library preparation and sequencing was performed by DeepSeq (University of Nottingham) according to SOLiD instructions. Sequence reads were mapped to the *H. volcanii* genome (accession numbers: CP001953-CP001957) using BioScope (version 1.3.1). Custom Perl scripts were used to calculate and plot replication profiles as described previously⁵. Deep sequencing data are available here: <http://www.ncbi.nlm.nih.gov/geo/query/acc.cgi?acc=GSE41961>

Identification of SNPs

Single nucleotide polymorphisms (SNPs) present at >50% prevalence and with a coverage of >10x (mean genome-wide coverage is ~150x) are shown in Extended Data Table 1. Five SNPs were identified in the strain lacking all chromosomal origins (H1546) and four of these SNPs are already present in the *oriC*⁺ parent strain (H53). The remaining SNP leads to a predicted glycine to valine change in the hypothetical protein HVO_A0627, this mutation is already present in the $\Delta oriC1,2$ parent (H1340). However, it is absent from its $\Delta oriC1::trpA^+ \Delta oriC2$ parent (H1293) and both these strains grow at near-identical rates (Source Data for Fig. 2c).

Isolation of *oriC3* by genetic screen for autonomously replicating sequences

We previously showed that genetic screens in *H. volcanii* isolate a single origin at a time, and that this can be circumvented by using origin deletion mutants⁴. Therefore, we deleted *oriC1* in a $\Delta ori-pHV1$ background, so that genetic screens would not be dominated by these two origins. Note that *ori-pHV1* was previously named *ori-pHV1/4*; this sequence hybridizes to two bands of ~690 kb and 86 kb on a pulsed field gel, which correspond in size to pHV4 and pHV1, respectively⁴. However, it is now clear that pHV4 has integrated on the main chromosome in laboratory strains, therefore *ori-pHV1/4* cannot be present on pHV4. Consequently, we have renamed this origin as *ori-pHV1* and renamed *ori-pHV4-2* as *ori-pHV4*. To delete *oriC1*, the *EcoRI-BspEI oriC1* duplex unwinding element (DUE) fragment of pTA441 was replaced with the *BamHI-XbaI hdrB*⁺ selectable marker from pTA187 to generate the *oriC1* deletion construct pTA946. Strain H300 was transformed with pTA946

as described previously³⁰, to generate the $\Delta oriC1::hdrB^+$ mutant H1023. Genomic DNA from strain H1023 was prepared as described previously³⁰, 25 μ g was partially digested with 0.5 units/ μ g of *AciI* for 30 minutes and fragments of 4-8 kb were ligated in the *ClaI* site of plasmid pTA131. One μ g of this genomic library was used to transform the recombination-deficient strain H112, plasmid DNAs from six transformants were passaged through *E. coli* and sequenced. All six clones contained the autonomously replicating *oriC3* region (pTA1100; Extended Data Fig. 3).

Identifying the integration of pHV4 into the main chromosome

Genomic DNA from wild isolate DS2 and laboratory strain H26 was digested with *ClaI*, *KpnI* or *NarI* (Extended Data Fig. 4). A Southern blot was probed with PCR products upstream (US; primers RFB5F and RFB3R) and downstream (DS; primers RFBF and RFBR) of the H26 profile discontinuity (Fig. 1b). The upstream 3646 bp *NarI* fragment and downstream 7478 bp *KpnI* fragment were isolated from H26 genomic libraries and cloned in pBluescript II SK+. The upstream clone pTA1238 and downstream clone pTA1236 contained chromosomal and pHV4 sequences (shown in Extended Data Fig. 4b), indicating that the entire 690 kb pHV4 had integrated into the main chromosome, by recombination between ISH18 insertion sequence elements HVO_0278 (chromosome) and HVO_A0279 (pHV4), as shown in Fig. 1d.

Deletion of *radA*

Deletion of *radA* was carried out as described previously²¹. Briefly, the $\Delta radA::trpA^+$ construct pTA324 was used for chromosomal deletion of *radA* as described previously³⁰, but in the presence of pTA411 for *in trans* complementation of *radA* to facilitate efficient homologous recombination. Deletion of *radA* results in slow growth, the fraction of slow-growing colonies ($\Delta radA$ candidates) that proved to be $\Delta radA$ was 94%, 100%, 43% and 12% for the wild-type, $\Delta oriC1$, $\Delta oriC2$ and $\Delta oriC3$ strains, respectively. Only a single $\Delta radA \Delta oriC1 \Delta oriC2 \Delta oriC3$ colony (1 of 70 screened) was recovered, this strain had undergone a chromosomal rearrangement involving the part of integrated pHV4 containing *ori-pHV4* (Extended Data Fig. 5). We were unable to delete *radA* from the strain lacking all chromosomal origins (0 of 455 slow-growing colonies screened).

Generating tryptophan-inducible *radA* strains

Plasmid pTA1343 carries a recombinant *radA* allele under control of the tryptophan-inducible *p.tnaA* promoter²². The *radA* gene was cloned downstream of the *p.tnaA* promoter in pTA927³³, from which a cassette comprising the t.L11e terminator, *p.tnaA* promoter, *radA* and t.Syn terminator was excised and linked to the *hdrB* marker from pTA187³⁰, whereupon it was inserted between the upstream and downstream flanking regions of *radA* in pTA131³⁰ to generate pTA1343 (Extended Data Fig. 6a). Further details are available upon request. pTA1343 was used to replace the native *radA* gene in H98 (wild-type, generating H1637) and H1608 ($\Delta oriC1,2,3,pHV4$, generating H1642) as described previously³⁰, except that transformants were plated on Hv-Ca+5-FOA containing 0.25 mM tryptophan to ensure expression of the *p.tnaA-radA*⁺ gene.

Supplementary Material

Refer to Web version on PubMed Central for supplementary material.

Acknowledgments

This work was supported through the Biotechnology and Biological Sciences Research Council (BB/E023754/1, BB/G001596/1). We thank the BBSRC for a David Phillips Fellowship awarded to CAN and Royal Society for a

University Research Fellowship awarded to TA, Ray Wilson for preparing libraries for sequencing, Alessandro de Moura and Iain Duggin for sharing unpublished data, and numerous colleagues for discussions.

References

1. Robinson NP, Bell SD. Origins of DNA replication in the three domains of life. *FEBS J.* 2005; 272:3757–3766. [PubMed: 16045748]
2. Hartman AL, et al. The complete genome sequence of *Haloflex volcanii* DS2, a model archaeon. *PLoS ONE.* 2010; 5:e9605. [PubMed: 20333302]
3. Leigh JA, Albers SV, Atomi H, Allers T. Model organisms for genetics in the domain Archaea: methanogens, halophiles, Thermococcales and Sulfolobales. *FEMS Microbiol Rev.* 2011; 35:577–608. [PubMed: 21265868]
4. Norais C, et al. Genetic and physical mapping of DNA replication origins in *Haloflex volcanii*. *PLoS Genet.* 2007; 3:e77. [PubMed: 17511521]
5. Müller CA, Nieduszynski CA. Conservation of replication timing reveals global and local regulation of replication origin activity. *Genome Res.* 2012; 22:1953–1962. [PubMed: 22767388]
6. Sernova NV, Gelfand MS. Identification of replication origins in prokaryotic genomes. *Briefings in Bioinformatics.* 2008; 9:376–391. [PubMed: 18660512]
7. de Moura AP, Retkute R, Hawkins M, Nieduszynski CA. Mathematical modelling of whole chromosome replication. *Nucleic Acids Res.* 2010; 38:5623–5633. [PubMed: 20457753]
8. Duggin IG, Dubarry N, Bell SD. Replication termination and chromosome dimer resolution in the archaeon *Sulfolobus solfataricus*. *EMBO J.* 2011; 30:145–153. [PubMed: 21113132]
9. Retkute R, Nieduszynski CA, de Moura A. Dynamics of DNA replication in yeast. *Physical Review Letters.* 2011; 107:068103. [PubMed: 21902372]
10. Duggin IG, McCallum SA, Bell SD. Chromosome replication dynamics in the archaeon *Sulfolobus acidocaldarius*. *Proc Natl Acad Sci USA.* 2008; 105:16737–16742. [PubMed: 18922777]
11. Skovgaard O, Bak M, Lobner-Olesen A, Tommerup N. Genome-wide detection of chromosomal rearrangements, indels, and mutations in circular chromosomes by short read sequencing. *Genome Res.* 2011; 21:1388–1393. [PubMed: 21555365]
12. Lindås AC, Bernander R. The cell cycle of archaea. *Nat Rev Microbiol.* 2013; 11:627–638. [PubMed: 23893102]
13. Dershowitz A, et al. Linear derivatives of *Saccharomyces cerevisiae* chromosome III can be maintained in the absence of autonomously replicating sequence elements. *Mol Cell Biol.* 2007; 27:4652–4663. [PubMed: 17452442]
14. Vujcic M, Miller CA, Kowalski D. Activation of silent replication origins at autonomously replicating sequence elements near the HML locus in budding yeast. *Mol Cell Biol.* 1999; 19:6098–6109. [PubMed: 10454557]
15. Vashee S, et al. Sequence-independent DNA binding and replication initiation by the human origin recognition complex. *Genes Dev.* 2003; 17:1894–1908. [PubMed: 12897055]
16. Kogoma T. Stable DNA replication: interplay between DNA replication, homologous recombination, and transcription. *Microbiol Mol Biol Rev.* 1997; 61:212–238. [PubMed: 9184011]
17. Kreuzer KN, Brister JR. Initiation of bacteriophage T4 DNA replication and replication fork dynamics: a review in the *Virology Journal* series on bacteriophage T4 and its relatives. *Virology J.* 2010; 7:358.
18. McGlynn P, Savery NJ, Dillingham MS. The conflict between DNA replication and transcription. *Mol Microbiol.* 2012; 85:12–20. [PubMed: 22607628]
19. McCready S, et al. UV irradiation induces homologous recombination genes in the model archaeon, *Halobacterium* sp. NRC-1. *Saline Systems.* 2005; 1:3. [PubMed: 16176594]
20. Woods WG, Dyall-Smith ML. Construction and analysis of a recombination-deficient (*radA*) mutant of *Haloflex volcanii*. *Mol Microbiol.* 1997; 23:791–797. [PubMed: 9157249]
21. Delmas S, Shunburne L, Ngo HP, Allers T. Mre11-Rad50 promotes rapid repair of DNA damage in the polyploid archaeon *Haloflex volcanii* by restraining homologous recombination. *PLoS Genet.* 2009; 5:e1000552. [PubMed: 19593371]

22. Large A, et al. Characterization of a tightly controlled promoter of the halophilic archaeon *Haloferax volcanii* and its use in the analysis of the essential *cct1* gene. *Mol Microbiol.* 2007; 66:1092–1106. [PubMed: 17973910]
23. Ogawa T, Pickett GG, Kogoma T, Kornberg A. RNase H confers specificity in the *dnaA*-dependent initiation of replication at the unique origin of the *Escherichia coli* chromosome *in vivo* and *in vitro*. *Proc Natl Acad Sci USA.* 1984; 81:1040–1044. [PubMed: 6322184]
24. Matsunaga F, et al. Genomewide and biochemical analyses of DNA-binding activity of Cdc6/Orc1 and Mcm proteins in *Pyrococcus* sp. *Nucleic Acids Res.* 2007; 35:3214–3222. [PubMed: 17452353]
25. Newman TJ, Mamun MA, Nieduszynski CA, Blow JJ. Replisome stall events have shaped the distribution of replication origins in the genomes of yeasts. *Nucleic Acids Res.* 2013 10.1093/nar/gkt728. [PubMed: 23963700]
26. Breuert S, Allers T, Spohn G, Soppa J. Regulated polyploidy in halophilic archaea. *PLoS ONE.* 2006; 1:e92. [PubMed: 17183724]
27. Storchova Z, et al. Genome-wide genetic analysis of polyploidy in yeast. *Nature.* 2006; 443:541–547. [PubMed: 17024086]
28. Rosenshine I, Tchelet R, Mevarech M. The mechanism of DNA transfer in the mating system of an archaeobacterium. *Science.* 1989; 245:1387–1389. [PubMed: 2818746]
29. McGeoch AT, Bell SD. Extra-chromosomal elements and the evolution of cellular DNA replication machineries. *Nat Rev Mol Cell Biol.* 2008; 9:569–574. [PubMed: 18523437]
30. Allers T, Ngo HP, Mevarech M, Lloyd RG. Development of additional selectable markers for the halophilic archaeon *Haloferax volcanii* based on the *leuB* and *trpA* genes. *Appl Environ Microbiol.* 2004; 70:943–953. [PubMed: 14766575]
31. Bryson V, Szybalski W. Microbial Selection. *Science.* 1952; 116:45–51.
32. Delmas S, Duggin IG, Allers T. DNA damage induces nucleoid compaction via the Mre11-Rad50 complex in the archaeon *Haloferax volcanii*. *Mol Microbiol.* 2013; 87:168–179. [PubMed: 23145964]
33. Allers T, Barak S, Liddell S, Wardell K, Mevarech M. Improved strains and plasmid vectors for conditional overexpression of His-tagged proteins in *Haloferax volcanii*. *Appl Environ Microbiol.* 2010; 76:1759–1769. [PubMed: 20097827]
34. Alkan C, et al. Personalized copy number and segmental duplication maps using next-generation sequencing. *Nat Genet.* 2009; 41:1061–1067. [PubMed: 19718026]
35. Pelve EA, Martens-Habbena W, Stahl DA, Bernander R. Mapping of active replication origins *in vivo* in thaum- and euryarchaeal replicons. *Mol Microbiol.* 2013 10.1111/mmi.12382. [PubMed: 23991938]
36. Mullakhanbhai MF, Larsen H. *Halobacterium volcanii* spec. nov., a Dead Sea halobacterium with a moderate salt requirement. *Arch Microbiol.* 1975; 104:207–214. [PubMed: 1190944]
37. Wendoloski D, Ferrer C, Dyall-Smith ML. A new simvastatin (mevinolin)-resistance marker from *Haloarcula hispanica* and a new *Haloferax volcanii* strain cured of plasmid pHV2. *Microbiology.* 2001; 147:959–964. [PubMed: 11283291]
38. Lestini R, Duan Z, Allers T. The archaeal Xpf/Mus81/FANCM homolog Hef and the Holliday junction resolvase Hjc define alternative pathways that are essential for cell viability in *Haloferax volcanii*. *DNA Repair.* 2010; 9:994–1002. [PubMed: 20667794]

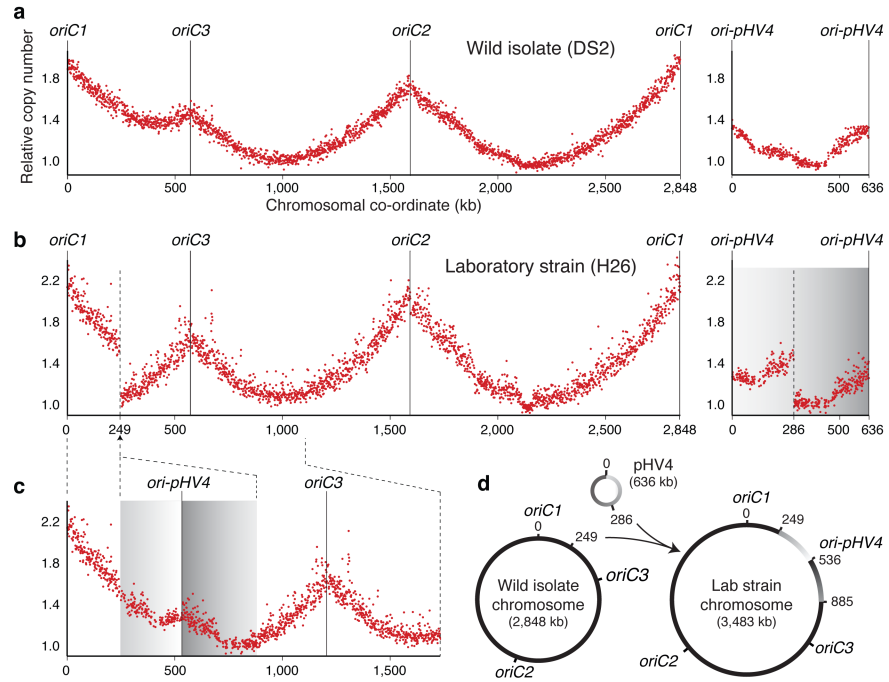


Figure 1. Replication profiles for *H. volcanii* wild isolate and laboratory strain
(a) Relative copy number plotted against chromosomal co-ordinate for the main chromosome and pHV4 of wild isolate DS2. Circular chromosomes are displayed linearized at position 0, vertical lines mark replication origins. **(b)** Sequence reads for laboratory strain H26 mapped to the reference genome (DS2). pHV4 shading reflects chromosomal co-ordinate. **(c)** Sequence reads for H26 mapped to a reconstructed assembly of the main chromosome with pHV4 integrated at ~249 kb. Grey shading from (b) indicates the orientation of pHV4 integration. **(d)** Integration of pHV4 into the main chromosome of H26.

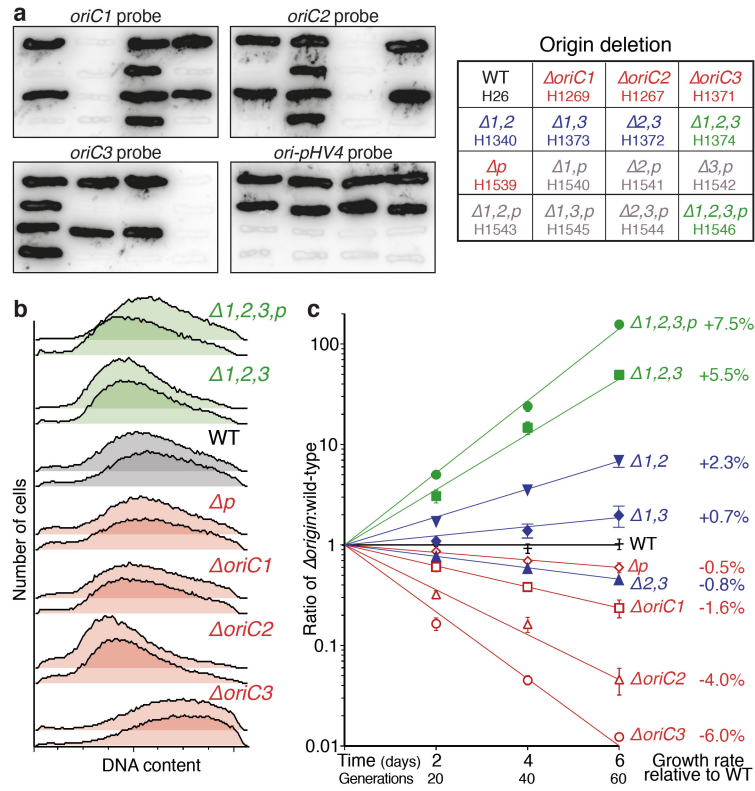


Figure 2. Characterization of origin deletion strains

(a) Deletion strains were confirmed by hybridization with origin-specific probes (“p” refers to *ori-pHV4*). (b) Flow cytometry was used to measure DNA content of origin deletion strains, biological replicates are shown; no differences in cell size were observed (data not shown). (c) Pairwise growth competition assays comparing wild-type (H54, *bgaHa*⁺) and origin deletion strains. The average and standard error of four independent replicates are plotted.

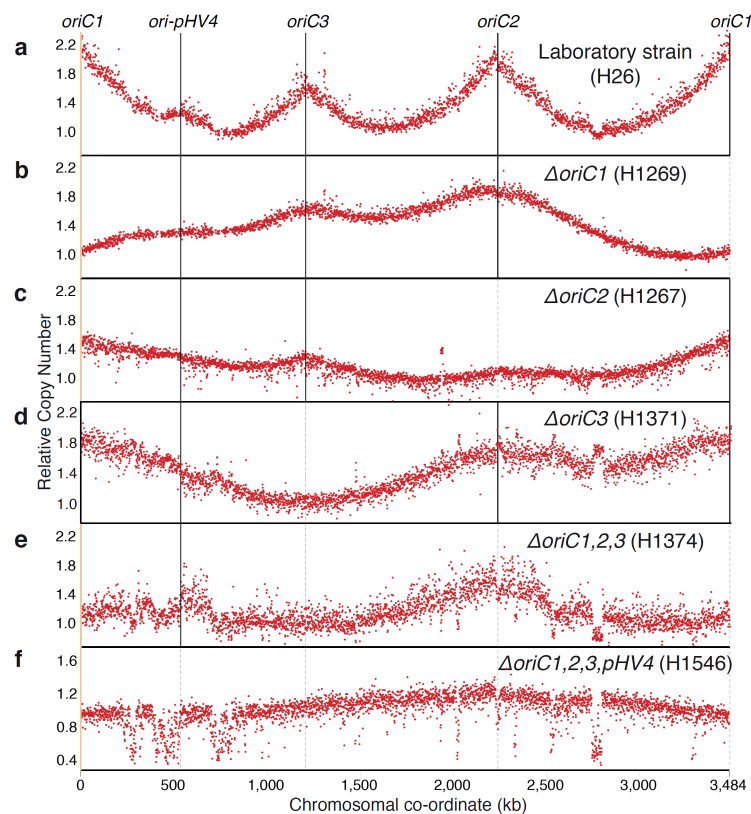


Figure 3. Origin deletion strain replication profiles

Comparison of replication profiles for (a) laboratory strain (wild type), (b) $\Delta oriC1$, (c) $\Delta oriC2$, (d) $\Delta oriC3$, (e) $\Delta oriC1,2,3$ and (f) $\Delta oriC1,2,3,pHV4$ mutants. Relative copy number for the main chromosome with integrated pHV4 was derived and displayed as in Fig. 1c, dashed lines mark the location of deleted origins.

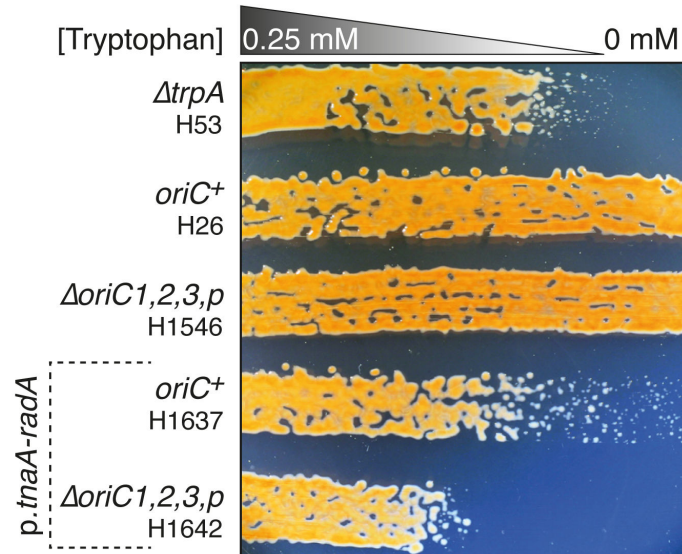


Figure 4. RadA recombinase is essential in an $\Delta oriC_{1,2,3,pHV4}$ mutant
radA was placed under control of the tryptophan-inducible *p.tnaA* promoter, in $oriC^+$ and $\Delta oriC_{1,2,3,pHV4}$ strains (H1637 and H1642). The former grows slowly in the absence of tryptophan while the latter is inviable. Absence of tryptophan does not affect the growth of $oriC^+$ and $\Delta oriC_{1,2,3,pHV4}$ control strains (H26 and H1546); the $\Delta trpA$ control strain (H53) is auxotrophic for tryptophan.